芳野裕子，海野光昭，西村美穂，中川慎一郎，大園秀一，上田耕一郎，原田なをみ，渡邊順子，松石豊次郎.	進行性の貧血を合併した5番染色体長腕中間部欠失症例.（ポスター）	第37回日本小児遺伝学会，名古屋市.	2014年4月10日（木）	国内
中林一彦、Court Franck，田山千春，Romanelli Valeria，副島英伸，和氣徳夫，Esteller Manel，緒方勤，秦健一郎，Monk David.	Genome-wide parent-of-origin DNA methylation analysis reveals the intricacies of the human imprintome and suggests a germline methylation independent control of imprinting in the placenta.（ポスター）	第8回日本エピジェネティクス研究会年会，東京大学	2014年5月25-27日.	国内
西岡憲一、Hitomi Miyazaki, Ken Higashimoto, Yukari Yada, Takaho A. Endo, Jafar Sharif, Manabu Nakayama, Hidenobu Soejima, Haruhiko Koseki, Susumu Hirose.	Ash1l methylates Lys36 of histone H3 independently of transcriptional elongation to counteract Polycomb silencing.（ポスター）	第8回日本エピジェネティクス研究会年会，東京大学	2014年5月25-27日.	国内
前田寿幸，Rumbajan Janette Mareska，東元健，中林一彦，八木ひとみ，秦健一郎，城圭一郎，副島英伸.	Beckwith-Wiedemann症候群と肝芽腫における multiple methylation defectの解析.（ポスター）	第8回日本エピジェネティクス研究会年会，東京大学	2014年5月25-27日.	国内
緒方怜奈，松岡幹，原口康平，チョン・ピンフィー，吉良龍太郎，渡邊順子，才津浩智.	GLUT1欠損症と考えられていたがエクソーム解析により乳児悪性焦点移動性部分発作と診断された一例.（ポスター）	第56回日本小児神経学会，浜松市.	2014年5月29-31日	国内
元島成信，原田なをみ，田中征治，芳野信，齋藤仲道，田中悦子，此元隆雄，中西浩一，松石豊次郎，渡邊順子.	フィンランド型先天性ネフローゼ症候群の出生前診.（ポスター）	第38回日本遺伝カウンセリング学会，川崎市.	2014年6月20-23日	国内

荻朋男.	DNA 修復機構の異常により発症する先天性疾患とゲノム不安定性/発がん. (口頭：教育講演)	第 20 回日本家族性腫瘍学会学術集会, 福島.	2014 年 6 月 13-14 日	国内
森本芳郎, 小野慎治, 黒滝直弘, 吉浦孝一郎, 小澤寛樹.	幻覚・妄想を呈した正常圧水頭症の家族例の遺伝学的考察. (口頭)	日本精神神経学会総会, パシフィコ横浜.	2014 年 6 月 26～28 日	国内
田代 恭子、石井 宏美、木下 幸恵、鈴谷 由吏、柳内 千尋、井上 かおり、稲場 美佐、青木 久美子、但馬 剛、依藤 亨、重松 陽介、猪口 隆洋、松石 豊次郎、渡邊 順子.	当施設で診断した軽症型プロピオン酸血症 7 症例の検討. (口頭)	第 41 回日本マススクリーニング学会, 広島市.	2014 年 8 月 22-23 日	国内
渡辺聡, 伊達木澄人, 近河日智, 中富明子, 木下英一, 吉浦孝一郎, 深見真紀, 緒方勤, 森内浩幸.	中枢神経奇形を合併した複合型下垂体機能低下症の 2 例 : trio exome 解析による新規原因遺伝子同定の試み. (口頭)	第 48 回小児内分泌学会学術集会, 浜松.	9 月 25～27 日	国内
原田なをみ、田中征治、芳野 信、齋藤仲道、田中悦子、此元隆雄、中西浩一、松石豊次郎、渡邊順子.	マイクロアレイ解析が有用であった 15 番染色体 q26 端部欠失の 1 例. (口頭)	第 21 回 遺伝性疾患に関する出生前診断研究会, 宮崎市.	2014 年 9 月 13 日	国内
石毛美夏、小川えりか、碓井ひろみ、米沢龍太、小平隆太郎、渡邊順子、渕上達夫、高橋昌里.	治療中に急性硬膜下出血をきたしたグルタル酸血症 I 型の 1 例. (ポスター)	第 56 回日本先天代謝異常学会, 仙台市.	2014 年 11 月 13-15 日	国内
鈴谷由吏、田代 恭子、稲場 美佐、青木 久美子、但馬 剛、依藤 亨、重松 陽介、猪口 隆洋、松石 豊次郎、渡邊 順子.	当施設で診断した軽症型プロピオン酸血症 7 症例の検討. (ポスター)	第 56 回日本先天代謝異常学会, 仙台市.	2014 年 11 月 13-15 日	国内

中島葉子，Judith Meijer, Doreen Dobritzsch、渡邊順子，久原とみ子，三渕 浩，李　知子，衞藤　薫，伊藤哲哉，Andre Van Kuilenburg.	β ウレイドプロピオナーゼ欠損症の臨床的・生化学的・分子生物学的検討と p.R326Q 変異頻度.（ポスター）	第 56 回日本先天代謝異常学会，仙台市.	2014 年 11 月 13-15 日	国内
Tomoo Ogi.	Molecular cloning and characterisation of new human DNA repair genes.（口頭）	3R Symposium Program（DNA 修復，組換え，修復）に関する国際会議，御殿場，静岡	2014 年 11 月 17～22 日	国内
Chaowan Guo, Yuka Nakazawa, Shimada Mayuko, Lisa Woodbine, Nan Jia, Kiyonobu Karata, Hitomi Miyazaki, Alan Lehmann, Penny A Jeggo & Tomoo Ogi.	Molecular characterization and functional analysis of XRCC4, a novel pathological gene for radiation sensitivity and developmental abnormalities.（口頭）	3R Symposium Program（DNA 修復，組換え，修復）に関する国際会議，御殿場，静岡	2014 年 11 月 17～22 日	国内
Yuka Nakazawa, Kazuya Kashiyama, Daniela T. Pilz, Chaowan Guo, Mayuko Shimada, Kensaku Sasaki, Heather Fawcett, Jonathan F. Wing, Susan O. Lewin, Lucinda Carr, Tao-Sheng Li, Koh-ichiro Yoshiura, Atsushi Utani, Akiyoshi Hirano, Danielle Greenblatt, Tiziana Nardo, Miria Stefanini, David McGibbon, Robert Sarkany, Hiva Fassihi, Norisato Mitsutake, Alan R. Lehmann & Tomoo Ogi.	ERCC1/XPF deficiency causes three NER-deficient disorders: a patient with various symptoms of xeroderma pigmentosum, Cockayne syndrome, and Fanconi anemia.（口頭）	3R Symposium Program（DNA 修復，組換え，修復）に関する国際会議，御殿場，静岡	2014 年 11 月 17～22 日	国内
朝重耕一，渡辺聡，三嶋博之，木下晃，松本桂太郎，及川将弘，宮崎拓郎，土谷智史，山崎直哉，福島喜代康，永安　武，吉浦孝一郎.	家族性肺がんにおける新規責任遺伝子の同定.（口頭）	第59回日本人類遺伝学会，タワーホール船堀，東京	2014 年 11 月 19 日～22 日	国内

三嶋博之，菊入　崇，三古谷　忠，木下晃，吉浦孝一郎.	多発性歯牙腫合併症例を含むSATB2遺伝子変異症候群の新規変異の同定．（口頭）	第59回日本人類遺伝学会，タワーホール船堀，東京	2014年11月19日～22日	国内
要 匡，柳久美子，澤田浩武，比嘉真紀，園田徹，成富研二.	Ohdo症候群オリジナル症例はKAT6B, MED12以外の遺伝子が原因である．（口頭）	第59回日本人類遺伝学会，タワーホール船堀，東京	2014年11月19日～22日	国内
渡辺　聡，伊達木　澄人，中富明子，木下　晃，朝重耕一，木下英一，三嶋博之，森内浩幸，吉浦孝一郎.	ddPCRを用い他McCune-Albright症候群のGNASモザイク変異検出の試み．（口頭）	第59回日本人類遺伝学会，タワーホール船堀，東京	2014年11月19日～22日	国内
森本芳郎，小野慎治，森貴俊，黒滝直弘，吉浦孝一郎，小澤寛樹.	Panic障害多発家系例に対するExome解析．（口頭）	第59回日本人類遺伝学会，タワーホール船堀，東京	2014年11月19日～22日	国内
森崎慎太郎，三浦清徳，東島　愛，阿部修平，三浦生子，長谷川ゆり，吉田　敦，金内優典，吉浦孝一郎，増崎英明.	母体血漿中への妊娠関連胎盤特異的microRNAの流入量および分娩後の消失速度と陣痛との関連について．（口頭）	第59回日本人類遺伝学会，タワーホール船堀，東京	2014年11月19日～22日	国内
島袋末美，渡嘉敷良乃，宮城郁乃，石原美紀，名護珠美，建山正男，比嘉真紀，仲宗根勇，要 匡.	次世代シーケンサを活用したHIVゲノム薬剤耐性関連遺伝子マイナーアリルの検出．（口頭）	第59回日本人類遺伝学会，タワーホール船堀，東京	2014年11月19日～22日	国内
東島　愛，三浦清徳，三嶋博之，木下　晃，塚本大空，阿部修平，長谷川ゆり，吉田　敦，吉浦孝一郎，増崎英明.	母体血と比較して胎児血で高発現するmicroRNAの同定．（口頭）	第59回日本人類遺伝学会，タワーホール船堀，東京	2014年11月19日～22日	国内
長谷川ゆり，三浦清徳，東島　愛，阿部修平，三浦生子，吉田　敦，金内優典，吉浦孝一郎，増崎英明.	母体血漿中miR-517aおよびmiR518bは前置胎盤に対する帝王切開時の出血量に関連する．（口頭）	第59回日本人類遺伝学会，タワーホール船堀，東京	2014年11月19日～22日	国内

渕　直樹，三浦清徳，東島　愛，長谷川ゆり，阿部修平，三浦生子，村上優子，三嶋博之，木下 晃，金内優典，吉浦孝一郎，増崎英明.	母体血漿中 cell-free microRNA 流入量と母体の body mass index および新生児出生体重との関連. （口頭）	第59回日本人類遺伝学会，タワーホール船堀，東京	2014 年 11 月 19 日～22 日	国内
村上優子，三浦清徳，東島　愛，長谷川ゆり，阿部修平，三浦生子，三嶋博之，木下　晃，金内優典，吉浦孝一郎，増崎英明.	双胎間輸血症候群発症予測における母胎血漿中胎盤特異的 cell-free mRNA の有用性に関する検討. （口頭）	第59回日本人類遺伝学会，タワーホール船堀，東京	2014 年 11 月 19 日～22 日	国内
阿部修平，三浦清徳，三浦生子，山崎健太郎，長谷川ゆり，東島　愛，吉田　敦，金内優典，吉浦孝一郎，増崎英明.	NILM/ASC-US 例における HPV-16 単独感染群と HPV-52 単独感染群の細胞診所見の変化. （口頭）	第59回日本人類遺伝学会，タワーホール船堀，東京	2014 年 11 月 19 日～22 日	国内
我那覇　章，要 匡.	CHD7 遺伝子の新規変異を認めた CHARGE 症候群の一例.（ポスター）	第59回日本人類遺伝学会，タワーホール船堀，東京	2014 年 11 月 19 日～22 日	国内
原田なをみ，田中征治，芳野　信，齋藤仲道，田中悦子，此元隆雄，中西浩一，松石豊次郎，渡邊順子.	マイクロアレイ解析が有用であった 15 番染色体 q26 端部欠失の 1 例.（ポスター）	第59回日本人類遺伝学会，タワーホール船堀，東京	2014 年 11 月 19 日～22 日	国内
副島英伸，Rumbajan Janette Mareska，畑田出穂，中林一彦，泰健一郎，青木茂久，関博之 竹田　省，城圭一郎.	Small for gestational age（SGA）胎盤のゲノムワイド DNA メチル化解析.（ポスター）	第59回日本人類遺伝学会，タワーホール船堀，東京	2014 年 11 月 19 日～22 日	国内
Hiroyuki Mishima, Koh-ichiro Yoshiura.	Handmaid Building of a High-Performance Computing Cluster and a Storage System for Bioinformatics. ポスター）	生命医薬情報学連合大会，仙台市仙台国際センター，仙台	2014 年 10 月 2～4 日	国内

荻朋男，中沢由華，勝木陽子，Alagoz Meryem，Kakarougkas Andreas，眞貝洋一，Jeggo Penny.	ヒストンH3K9メチル化酵素類のDNA二重鎖切断修復反応への関与.（口頭）	第87回日本生化学会大会 シンポジウム，京都	2014年10月15～18日	国内
荻朋男.	転写共役ヌクレオチド除去修復の開始反応の分子機構.（口頭）	日本放射線影響学会第57回大会 ワークショップ，鹿児島	2014年10月1～3日.	国内
筒井正人，久保田陽秋，野口克彦，松崎俊博，坂梨まゆ子，喜名美香，内田太郎，仲宗根淳子，要匡，須加原一博，垣花学.	一酸化窒素合成酵系の遺伝子欠損はマウス中大脳動脈閉塞後梗サイズを著明に縮小させる.（口頭）	第67回日本薬理学会，西南部会，産業医科大学ラマツィーニホール，北九州	2014年11月23日	国内
Tadashi Kaname, Chang-Seok Ki, Norio Niikawa, George S. Baillie, Jonathan P. Day, Gen Nishimura, Nobuo Mastuura, Kumiko Yanagi, Kenji Naritomi, Miles D. Houslay, Sung Yoon Cho, Dong-Kyu Jin.	Molecular pathology of acrodysostosis without hormone resistance caused by heterozygous mutations in cAMP phosphodiesterase-4D.（ポスター）	第37回日本分子生物学会年会，パシフィコ横浜，横浜	2014年11月25日～27日	国内
安田武嗣，香川亘，齋藤健吾，荻朋男，花岡文雄，菅澤薫，胡桃坂仁志，田嶋克史.	ヒトRAD52タンパク質のアセチル化制御.（ポスター）	第37回日本分子生物学会年会，パシフィコ横浜，横浜	2014年11月25日～27日	国内
唐田清伸，郭朝万，荻朋男.	転写と共役したヌクレオチド除去修復のin vitro反応系の構築.（ポスター）	第37回日本分子生物学会年会，パシフィコ横浜，横浜	2014年11月25日～27日	国内
香川亘，五月女美香，齋藤健吾，安田武嗣，荻朋男，胡桃坂仁志.	ヒトRAD52タンパク質における二つのDNA結合部位の役割.（ポスター）	第37回日本分子生物学会年会，パシフィコ横浜，横浜	2014年11月25日～27日	国内

宮崎仁美，荻 朋男.	コケイン症候群様の臨床症状を示す遺伝性疾患の責任遺伝子探索.（ポスター）	第37回日本分子生物学会年会，パシフィコ横浜，横浜	2014年11月25日～27日	国内
嶋田繭子，荻 朋男.	エキソーム解析を用いたDNA修復機構欠損性疾患の新規責任遺伝子の探索.（ポスター）	第37回日本分子生物学会年会，パシフィコ横浜，横浜	2014年11月25日～27日	国内
丹伊田 浩行，松沼 亮一，荻 朋男，森脇 真一，北川 雅敏.	DDB2-dependent HBO1 recruitment is essential for repair of UV-induced cyclobutane pyrimidine dimmer.（口頭）	第37回日本分子生物学会年会，パシフィコ横浜，横浜	2014年11月25日～27日	国内
中沢由華，郭朝万，嶋田繭子，宮崎 仁美，唐田 清伸，荻 朋男.	放射線感受性および各種発達異常を示す遺伝性疾患の新規責任遺伝子の同定と分子機能解析.（口頭）	第37回日本分子生物学会年会，パシフィコ横浜，横浜	2014年11月25日～27日	国内
八戸由佳子，田中玄師，田中征治，渡邊順子，松石豊次郎，長井孝二郎，坂本照夫，岡田純一郎.	学童期の急性発作に対し血液浄化療法が有効であったメープルシロップ尿症の1例.（口頭）	第482回日本小児科学会，福岡地方会，久留米市	2014年12月13日	国内

2．学会誌・雑誌等における論文掲載雑誌

発表者氏名	論文タイトル名	発表誌名	発表した時期	国内・外の別
Jia N, Nakazawa Y, Guo C, Shimada M, Sethi M, Takahashi Y, Ueda H, Nagayama Y & Ogi T.	A rapid comprehensive assay system for DNA repair activity and cytotoxic effects of DNA damaging reagents by measuring unscheduled DNA synthesis and recovery of RNA synthesis after DNA damage.	***Nature Protocols***	10(1): 12-24, 2015.	国外

Kaname T, Ki CS, Niikawa N, Baillie GS, Day JP, Yamamura KI, Ohta T, Nishimura G, Mastuura N, Kim OH, Sohn YB, Kim HW, Cho SY, Ko AR, Lee JY, Kim HW, Ryu SH, Rhee H, Yang KS, Joo K, Lee J, Kim CH, Cho KH, Kim D, Yanagi K, Naritomi K, Yoshiura KI, Kondoh T, Nii E, Tonoki H, Houslay MD, Jin DK.	Heterozygous mutations in cyclic AMP phosphodiesterase-4D (PDE4D) and protein kinase A (PKA) provide new insights into the molecular pathology of acrodysostosis.	***Cell Signaling***	26(11): 2446-2459, 2014.	国外
Baple E.L., Chambers H., Cross H.E., Fawcett H., Nakazawa Y., Chioza B.A., Harlalka G.V., Mansour S., Sreekantan-Nair A., Patton M.A., Muggenthaler M., Rich P., Wagner K., Coblentz R., Stein C.K., Last J.I., Taylor A.M., Jackson A.P., Ogi T., Lehmann A.R., Green C.M. & Crosby A.H.	Hypomorphic PCNA mutation underlies a human DNA repair disorder.	***Journal of Clinical Investigation***	124(7): 3137-3146, 2014.	国外
Nagata E, Kano H, Kato F, Yamaguchi R, Nakashima S, Takayama S, Kosaki R, Tonoki H, Mizuno S, Watanabe S, Yoshiura KI, Kosho T, Hasegawa T, Kimizuka M, Suzuki A, Shimizu K, Ohashi H, Haga N, Numabe H, Horii E, Nagai T, Yoshihashi H, Nishimura G, Toda T, Takada S, Yokoyama S, Asahara H, Sano S, Fukami M, Ikegawa S, Ogata T.	Japanese founder duplications/triplications involving BHLHA9 are associated with split-hand/foot malformation with or without long bone deficiency and Gollop-Wolfgang complex.	***Orphanet Journal of Rare Diseases***	9(1): 125, 2014.	国外

Miura K, Morisaki S, Abe S, Higashijima A, Hasegawa Y, Miura S, Tateishi S, Mishima H, Yoshiura K, Masuzaki H.	Circulating levels of maternal plasma cell-free pregnancy-associated placenta-specific microRNAs are associated with placental weight.	***Placenta***	35(10): 848-851, 2014.	国外
Miura K, Hasegawa Y, Abe S, Higashijima A, Miura S, Mishima H, Kinoshita A, Kaneuchi M, Yoshiura K, Masuzaki H.	Clinical applications of analysis of plasma circulating complete hydatidiform mole pregnancy-associated miRNAs in gestational trophoblastic neoplasia: A preliminary investigation.	***Placenta***	35(9): 787-798, 2014.	国外
Miura K, Mishima H, Kinoshita A, Hayashida C, Abe S, Tokunaga K, Masuzaki H, Yoshiura KI.	Genome-wide association study of HPV-associated cervical cancer in Japanese women.	***Journal of Medical Virology***	86(7): 1153-1158, 2014.	国外
Matsumoto H, Tsuchiya T, Yoshiura K, Hayashi T, Hidaka S, Nanashima A, Nagayasu T.	ABCC11/MRP8 Expression in the Gastrointestinal Tract and a Novel Role for Pepsinogen Secretion.	***Acta Histochemica et Cytochemica***	47(3): 85-94, 2014.	国外
Tsurusaki Y, Koshimizu E, Ohashi H, Phadke S, Kou I, Shiina M, Suzuki T, Okamoto N, Imamura S, Yamashita M, Watanabe S, Yoshiura K, Kodera H, Miyatake S, Nakashima M, Saitsu H, Ogata K, Ikegawa S, Miyake N, Matsumoto N.	De novo SOX11 mutations cause Coffin-Siris syndrome.	***Nat. Commun.***	5: 4011, 2014.	国外

Miura K, Higashijima A, Miura S, Mishima H, Yamasaki K, Abe S, Hasegawa Y, Kaneuchi M, Yoshida A, Kinoshita A, Yoshiura K, Masuzaki H.	Predominantly placenta-expressed mRNAs in maternal plasma as predictive markers for twin-twin transfusion syndrome.	***Prenat. Diagn.***	34(4): 345-349, 2014.	国外
Abe S, Miura K, Kinoshita A, Mishima H, Miura S, Yamasaki K, Hasegawa Y, Higashijima A, Jo O, Yoshida A, Kaneuchi M, Yoshiura K, Masuzaki H.	Single human papillomavirus 16 or 52 infection and later cytological findings in Japanese women with NILM or ASC-US.	***J. Hum. Genet.***	59(5): 251-255, 2014.	国外
Amani D, Khalilnezhad A, Ghaderi A, Niikawa N, Yoshiura KI.	Transforming growth factor beta1 (TGFβ1) polymorphisms and breast cancer risk.	***Tumour Biol.***	35(5): 4757-4764.	国外
Tsukamoto O, Miura K, Mishima H, Abe S, Kaneuchi M, Higashijima A, Miura S, Kinoshita A, Yoshiura K, Masuzaki H.	Identification od endometrioid endometrial carcinoma-associated microRNA in tissue and plasma.	***Gynecol. Oncol.***	132(3): 715-721, 2014	国外
Ganaha A, Kaname T, Akazawa Y, Higa T, Shinnjou A, Naritomi K, Suzuki M.	Identification of two novel mutations in the NOG gene associated with congenital stapes ankylosis and symphalangism.	***J Hum Genet***	60(1): 27-34, 2015.	国外
Horai S, Yanagi K, Kaname T, Yamamoto M, Watanabe I, Ogura G, Abe S, Tanabe S, Furukawa T.	Establishment of a Primary Hepatocyte Culture from the Small Indian Mongoose (Herpestes auropunctatus) and Distribution of Mercury in Liver Tissue.	***Ecotoxycology***	23(9): 1681-1689, 2014.	国外

Kaname T, Yanagi K, Naritomi K.	A commentary on the promise of whole-exome sequencing in medical genetics.	***J Hum Genet***	59(3): 117-118, 2014.	国外
Ohnishi K, Semi K, Yamamoto T, Shimizu M, Tanaka A, Mitsunaga K, Okita K, Osafune K, Arioka Y, Maeda T, Soejima H, Moriwaki H, Yamanaka S, Woltjen K, Yamada Y.	Premature termination of reprogramming *in vivo* leads to cancer development through altered epigenetic regulation.	***Cell***	156(4): 663-677, 2014.	国外
Court F, Tayama C, Romanelli V, Martin-Trujillo A, Iglesias-Platas I, Okamura K, Sugahara N, Simón C, Moore H, Harness JV, Keirstead H, Sanchez-Mut JV, Kaneki E, Lapunzina P, Soejima H, Wake N, Esteller M, Ogata T, Hata K, Nakabayashi K, Monk D.	Genome-wide parent-of-origin DNA methylation analysis reveals the intricacies of the human imprintome and suggests a germline methylation independent establishment of imprinting.	***Genome Res***	24(4): 554-569, 2014.	国外
Higashimoto K, Jozaki K, Kosho T, Matsubara K, Fuke T, Yamada D, Yatsuki H, Maeda T, Ohtsuka Y, Nishioka K, Joh K, Koseki H, Ogata T, Soejima H.	A novel de novo point mutation of the OCT-binding site in the IGF2/H19-imprinting control region in a Beckwith-Wiedemann syndrome patient.	***Clin Genet***	86(6): 539-544, 2014.	国外

Maeda T, Higashimoto K, Jozaki K, Yatsuki H, Nakabayashi K, Makita Y, Tonoki H, Okamoto N, Takada F, Ohashi H, Migita M, Kosaki R, Matsubara K, Ogata T, Matsuo M, Hamasaki Y, Ohtsuka Y, Nishioka K, Joh K, Mukai T, Hata K, Soejima H.	Comprehensive and quantitative multilocus methylation analysis reveals the susceptibility of specific imprinted differentially methylated regions (DMRs) to aberrant methylation in Beckwith-Wiedemann syndrome with epimutations.	***Genet Med***	16(12): 903-912, 2014.	国外
Takama Y, Kubota A, Nakayama M, Higashimoto K, Jozaki K, Soejima H.	Fibroadenoma in Beckwith–Wiedemann syndrome with paternal uniparental disomy of chromosome 11p15.5.	***Pediatr Int***	56(6): 931-934, 2014.	国外
Nakajima Y, Meijer J, Dobritzsch D, Ito T, Meinsma R, Abeling NG, Roelofsen J, Zoetekouw L, Watanabe Y, Tashiro K, Lee T, Takeshima Y, Mitsubuchi H, Yoneyama A, Ohta K, Eto K, Saito K, Kuhara T, van Kuilenburg AB.	Clinical, biochemical and molecular analysis of 13 Japanese patients with β-ureidopropionase deficiency demonstrates high prevalence of the c.977G > A (p.R326Q) mutation.	***J Inherit Metab Dis.***	37(5): 801-812, 2014.	国外
Ikewaki N, Sonoda T, Migita H.	Modulation of CD93 molecule in a human monocyte-like cell line (U937) treated with nikel.	***J. of Kushu Univ. of Health and Welfare***	15: 129-137, 2014.	国内
三嶋博之	UCSC ゲノムブラウザ，今日から使えるデータベース・ウェブツール達人になるための実践ガイド 100	実験医学増刊	32(20): 3223-3225, 2014.	国内

三嶋博之	さまざまなヒトバリエーションデータベース	実験医学増刊	32(20): 3341-3343, 2014.	国内
要匡	Aarskog-Scott 症候群	日本臨床	別冊　神経症候群 IV: 434-436, 2014.	国内
要匡	鎖骨頭蓋形成不全症	日本臨床	別冊　神経症候群 IV: 725-726, 2014.	国内
大場隆，片渕秀隆，副島英伸	間葉性異形成胎盤 Placental mesenchymal dysplasia (PMD) の診断と原因遺伝子	病理と臨床	32(5): 535-540, 2014.	国内
副島英伸	インプリンティング疾患のエピジェネティクス	エピジェネティクスの産業応用，シーエムシー出版	266-279, 2014	国内
東元健，副島英伸	Beckwith-Wiedeman 症候群	日本臨床	別冊　神経症候群 IV: 498-501, 2014.	国内
東元健，副島英伸	Silver-Russell 症候群	日本臨床	別冊　神経症候群 IV : 685-688, 2014.	国内

VI. 主な研究成果の刊行物・別冊

Cellular Signalling 26 (2014) 2446–2459

Contents lists available at ScienceDirect

Cellular Signalling

journal homepage: www.elsevier.com/locate/cellsig

Heterozygous mutations in cyclic AMP phosphodiesterase-4D (PDE4D) and protein kinase A (PKA) provide new insights into the molecular pathology of acrodysostosis

Tadashi Kaname [a,1], Chang-Seok Ki [b,1], Norio Niikawa [c], George S. Baillie [d], Jonathan P. Day [e], Ken-ichi Yamamura [f], Tohru Ohta [g], Gen Nishimura [h], Nobuo Mastuura [i], Ok-Hwa Kim [j], Young Bae Sohn [k], Hyun Woo Kim [l], Sung Yoon Cho [m], Ah-Ra Ko [n], Jin Young Lee [n], Hyun Wook Kim [o], Sung Ho Ryu [o,p], Hwanseok Rhee [q], Kap-Seok Yang [q], Keehyoung Joo [r,s], Jooyoung Lee [r,s,t], Chi Hwa Kim [u], Kwang-Hyun Cho [v], Dongsan Kim [v], Kumiko Yanagi [a], Kenji Naritomi [a], Ko-ichiro Yoshiura [w], Tatsuro Kondoh [x], Eiji Nii [y], Hidefumi Tonoki [z], Miles D. Houslay [aa], Dong-Kyu Jin [m,*]

[a] Department of Medical Genetics, University of the Ryukyus Graduate School of Medicine, Okinawa, Japan
[b] Department of Laboratory Medicine and Genetics, Sungkyunkwan University School of Medicine, Seoul, Republic of Korea
[c] Health Sciences University of Hokkaido, Hokkaido, Japan
[d] Institute of Cardiovascular and Medical Sciences, College of Medical, Veterinary and Life Sciences, University of Glasgow, UK
[e] Department of Genetics, University of Cambridge, Cambridge, UK
[f] Division of Developmental Genetics, Institute of Resource Development and Analysis, Kumamoto University, Kumamoto, Japan
[g] Research Institute of Personalized Health Sciences, Health Sciences University of Hokkaido, Hokkaido, Japan
[h] Department of Pediatric Imaging, Tokyo Metropolitan Children's Medical Center, Tokyo, Japan
[i] Seitoku University, Chiba, Japan
[j] Department of Radiology, Gachon University Gil Medical Center, Incheon, Republic of Korea
[k] Department of Medical Genetics Ajou University Hospital, Ajou University School of Medicine, Suwon, Republic of Korea
[l] Department of Orthopedic Surgery, Yonsei University College of Medicine, Seoul, Republic of Korea
[m] Department of Pediatrics Samsung Medical Center, Sungkyunkwan University School of Medicine, Seoul, Republic of Korea
[n] Clinical Research Center, Samsung Biomedical Research Institute, Seoul, Republic of Korea
[o] Department of Life Sciences, Pohang University of Science and Technology, Pohang, Republic of Korea
[p] Division of Integrative Biosciences and Biotechnology and School of Interdisciplinary Bioscience and Bioengineering, Pohang University of Science and Technology, Pohang, Republic of Korea
[q] Macrogen Inc., Seoul, Republic of Korea
[r] Center for In Silico Protein Science, Korea Institute for Advanced Study, Republic of Korea
[s] Center for Advanced Computation, Korea Institute for Advanced Study, Republic of Korea
[t] School of Computational Sciences, Korea Institute for Advanced Study, Republic of Korea
[u] Mogam Biotechnology Research Institute, Yongin, Republic of Korea
[v] Department of Bio and Brain Engineering, Korea Advanced Institute of Science and Technology (KAIST), Republic of Korea
[w] Department of Human Genetics, Nagasaki University Graduate School of Biomedical Sciences, Nagasaki, Japan
[x] Division of Developmental Disabilities, The Misakaenosono Mutsumi Developmental, Medical and Welfare Center, Isahaya, Japan
[y] Department of Orthopaedic Surgery, Mie Prefectural Kusanomi Rehabilitation Center, Tsu, Japan
[z] Section of Clinical Genetics, Department of Pediatrics, Tenshi Hospital, Sapporo, Japan
[aa] Institute of Pharmaceutical Science, King's College, London, UK

ARTICLE INFO

Article history:
Received 14 June 2014
Received in revised form 16 July 2014
Accepted 16 July 2014
Available online 24 July 2014

Keywords:
Acrodysostosis

ABSTRACT

Acrodysostosis without hormone resistance is a rare skeletal disorder characterized by brachydactyly, nasal hypoplasia, mental retardation and occasionally developmental delay. Recently, loss-of-function mutations in the gene encoding cAMP-hydrolyzing phosphodiesterase-4D (*PDE4D*) have been reported to cause this rare condition but the pathomechanism has not been fully elucidated. To understand the pathogenetic mechanism of *PDE4D* mutations, we conducted 3D modeling studies to predict changes in the binding efficacy of cAMP to the catalytic pocket in PDE4D mutants. Our results indicated diminished enzyme activity in the two mutants we analyzed (Gly673Asp and Ile678Thr; based on PDE4D4 residue numbering). Ectopic expression of PDE4D mutants in HEK293 cells demonstrated this reduction in activity, which was identified by increased cAMP levels. However,

* Corresponding author at: Department of Pediatrics, Samsung Medical Center, Sungkyunkwan University School of Medicine, Samsung Medical Center, 50 Irwon-dong, Gangnam-gu, Seoul 135-710, Republic of Korea. Tel.: +82 2 3410 3525; fax: +82 2 3410 0043.
E-mail address: jindk@skku.edu (D.-K. Jin).
[1] The first two authors (T.K. and C.-S.K.) contributed equally to this work.

http://dx.doi.org/10.1016/j.cellsig.2014.07.025
0898-6568/

PDE4D
cAMP
Knok out rat

the cells from an acrodysostosis patient showed low cAMP accumulation, which resulted in a decrease in the phosphorylated cAMP Response Element-Binding Protein (pCREB)/CREB ratio. The reason for this discrepancy was due to a compensatory increase in expression levels of PDE4A and PDE4B isoforms, which accounted for the paradoxical decrease in cAMP levels in the patient cells expressing mutant isoforms with a lowered PDE4D activity. Skeletal radiographs of 10-week-old knockout (KO) rats showed that the distal part of the forelimb was shorter than in wild-type (WT) rats and that all the metacarpals and phalanges were also shorter in KO, as the name acrodysostosis implies. Like the G-protein α-stimulatory subunit and PRKAR1A, PDE4D critically regulates the cAMP signal transduction pathway and influences bone formation in a way that activity-compromising *PDE4D* mutations can result in skeletal dysplasia. We propose that specific inhibitory PDE4D mutations can lead to the molecular pathology of acrodysostosis without hormone resistance but that the pathological phenotype may well be dependent on an over-compensatory induction of other PDE4 isoforms that can be expected to be targeted to different signaling complexes and exert distinct effects on compartmentalized cAMP signaling.

1. Introduction

Acrodysostosis is a group of rare skeletal disorders characterized by brachydactyly, nasal hypoplasia, mental retardation, and occasionally developmental delay [1]. Progressive growth failure, short stature, and severe mid-face hypoplasia with skull deformity are common features of this disorder [1,2]. Acrodysostosis is phenotypically heterogeneous, and at least two groups are recognized: acrodysostosis with hormone resistance (OMIM #101800) and without hormone resistance (OMIM #614613). Acrodysostosis has attracted attention because the disorder shares common skeletal changes with Albright's hereditary osteodystrophy (AHO) or pseudohypoparathyroidism type 1a (PHP-1a). However, neither the biochemical impairment of the activity of G-protein α-stimulatory subunit (GNAS), which activates adenylyl cyclase and cAMP production [3], nor the genetic mutation of GNAS associated with PHP-1a, have been observed in individuals with acrodysostosis [1,4]. Recently, 3 patients with acrodysostosis with hormone resistance were identified to harbor the same nonsense mutation in the *PRKAR1A* gene [5]. The *PRKAR1A* gene encodes the cAMP-binding regulatory subunit of protein kinase A (PKA) that, together with an exchange protein activated by cAMP (Epac) [6], functions as a key intracellular signal transducer in Gsα-cAMP signaling.

Cyclic AMP levels are dynamically regulated not only by the activation of adenylyl cyclase but also by the inhibition of cAMP phosphodiesterases (PDEs), which provide the sole route for inactivation of this second messenger in the cells [7,8]. Of the PDE superfamily, selective inhibitors of the cAMP-specific phosphodiesterase-4 (PDE4) family have been shown to have profound anti-inflammatory actions [9–11] and have demonstrable therapeutic utility in both COPD (roflumilast) [12–14] and psoriatic arthritis (apremilast) [15,16].

Four genes encode the PDE4 family (PDE4A, PDE4B, PDE4C, PDE4D) with alternative splicing generating >20 isoforms [7,17]. A key functional consequence of this diversity is that various signaling scaffold and other proteins are able to sequester specific PDE4 isoforms [7, 18–20]. This tethering leads to the spatial localization of individual types of PDE4 isoforms which act to underpin compartmentalized cAMP signaling by shaping gradients of cAMP in distinct intracellular locales [7]. This ability confers non-redundant functional roles on specific PDE4 isoforms as uncovered using dominant negative [21–24] and siRNA (small interfering RNA)-mediated knockdown [25] approaches. In this, PDE4A1 provides the paradigm for PDE targeting [26–28], while PDE4D5 provides the paradigm for a particular PDE isoform being able to regulate a specific cellular function through targeting [29].

Individual PDE4 isoforms have distinct, intronic promoters that confer cell-type specific patterns of expression. Although little is known about these it has been shown that sustained changes in cAMP levels can alter expression levels of particular PDE4 isoforms, some of which have CRE loci that allows for their regulation by PKA phosphorylated CREB [30–33].

PDE4 isoforms are sub-categorized into long forms with UCR1 and UCR2 regulatory regions; short forms lacking UCR1 and super short forms lacking UCR1 but with a truncated UCR2 [7,34]. When cAMP levels are elevated in cells, the long PDE4 isoforms play a pivotal and exclusive role in determining both the magnitude and duration of this response through their activation through phosphorylation by cAMP-dependent protein kinase A (PKA) [35–43].

PDE4 long isoforms thus play a key role in underpinning both the cellular desensitization to cAMP as well as determining the compartmentalization of cAMP signaling. As such, changes in their activity, localization, post-translational regulation and the complement of different isoforms expressed in a particular cell are set to have profound physiological consequences [7].

Here, we present data collected using 3 approaches. First, in a mutation study, we identified 7 patients with acrodysostosis without hormonal resistance, linking the disease with the gene for cAMP-specific phosphodiesterase 4D (PDE4D). Second, in functional studies, we analyzed the 3D structure of PDE4D mutants and measured the activity of PDE4D mutants transfected into heterologous cells; we also colocalized PDE4D and β-arrestin using confocal microscopy and determined PDE4 activity and isoform expression in patient cells. Third, we generated PDE4D knockout (KO) rats and demonstrated that PDE4D loss results in the skeletal dysplasia phenotype observed in acrodysostosis. This work opens up a new horizon in the pathogenesis of acrodysostosis by showing that acrodysostosis without hormone resistance can be caused by alterations in cAMP degradation by PDE4D [7] and results in skeletal dysplasia.

2. Methods

2.1. Patient enrolment

Seven patients diagnosed as acrodysostosis without hormone resistance were included in the study. The patients represent all of the available patients diagnosed at the time of the study in Korea and Japan. Diagnosis was made by the typical X-ray features and the confirmation of the absence of the hormone resistance. The details of clinical features including hormone profiles are described in Table 1. One patient diagnosed as acrodysostosis without hormone resistance, who harbor the *PRKAR1A* mutation was included in the functional study for comparison.

The clinical features of 1 Korean (patient 2) and 3 Japanese patients (patients 4, 5 and 7) were described previously [44–46]. The mother of the Japanese siblings (patients 4 and 5) was reported to be affected mildly. For the other patients, clinical features are summarized in Table 1. Informed consent was obtained from the parents of all patients and this study was approved by the Institutional Review Board.

2.2. DNA study

Exome sequencing was performed on 2 Korean patients and 2 Japanese siblings with acrodysostosis (4 patients in 3 families), as well

Table 1
Clinical and laboratory findings of patients
Identifying mutations in acrodysostosis patients. Exomes were sequenced in 8 patients with acrodysostosis. We found that patient 8 had a de novo p.Arg368* mutation in *PRKAR1A*. When we compared the gene lists from patients other than patient 8, *PDE4D* was identified as the only gene they all shared.

	Patient 1	Patient 2	Patient 3	Patient 4	Patient 5	Patient 6	Patient 7	Patient 8	Reference range
Previous reports	Unpublished	Ref 9	Unpublished	Ref 8	Ref 8	Unpublished	Ref 10	Unpublished	
Gene	*PDE4D*	*PDE4D*	*PDE4D*	*PDE4D*	*PDE4D*	*PDE4D*	*PDE4D*	*PRKAR1A*	
Mutation	c.2033 T > C (p.I678T)	c.2018G > A (p.G673D)	c.2033 T > C (p.I678T)	c.683A > C (p.Q228P)	c.683A > C (p.Q228P)	c.689 T > C (p.L230S)	c.1759A > G (p.T587A)	c.1101C > T (p.R368X)	
Clinical findings									
GA (wk)/ Bwt (kg)	40/2.8	40/2.9	41/2.3	40/2.22	40/2.35	41/2.5	38/2.3	37 + 4/2.08	
Sex/age (y)	F/17 y	M/17 y	M/4 y 11 m	F/39 y	M/37 y	M/10 y 5m	F/8 y 5 m	M/3 y 9 m	
Height (cm)/ SD	144.7/−3.1	155/−2.8	98.8/−1.4	149/-2.1	135/-5.9	137.2/-0.9	131.6/-0.2	95.6/−1.7	
Weight (kg)/ SD	54/−0.1	57/−0.7	15/-1.6	54.3/0	42.3/-2.2	37.2/-0.6	31/0.2	15.7/−0.6	
Short nose with flat nasal bridge	+ (Nose vestigial)	+ (Nose vestigial)	+	+ (Nose vestigial)	+ (Nose vestigial)	+ (Nose vestigial)	+ (Nose vestigial)	+	
Prominent forehead	+	+	+	+	+	+	+	+	
Iris color at infancy*	Light brown	Black	Gray	Gray	Gray	Gray	Gray > brown	Gray	
Mental retardation	Mild	Severe	Severe	Severe	Severe	Mild to Severe	Severe	Mild	
Developmental milestone	Delayed	Delayed	Delayed	Delayed	Delayed	Delayed	Delayed	Normal	
Radiologic findings									
Peripheral skeletal dysplasia	Severe	Severe	Severe	Severe	Severe	Severe	Severe	Mild	
Nasomaxillary hypoplasia	Severe	Severe	Severe	Severe	Severe	Severe	Severe	Mild	
Brachydactyly	Severe	Severe	Severe	Severe	Severe	Severe	Severe	Mild	
Advanced bone age	Yes	Yes	Yes	Yes	Yes	Yes	Yes	Yes	
Laboratory findings									
Hormonal resistance	No	No	No	No	No	No	No	Yes	
PTH/Ca/P	34/9.8/3	9/4.1	NA/10.2/4.5	64.4/9.4/3.2	61.7/9.3/3.4	41/9.6/4.4	NA/9.8/5.3	56/9.5/5.0	PTH: 11–62 pg/ml Ca: 8.4–10.2 mg/dl P: 2.5–4.5 mg/dl
25-vit. D	15.29	NA	NA	NA	NA	NA	NA	34.52	8–51.9 mg/dl
fT4/TSH	1.54/2.25	1.17/0.91	1.5/1.54	1.25/1.25	1.26/0.41	1.6/1.79	1.15/NA	0.98/67.51	fT4: 0.89–1.8 ng/dl TSH: 0.35–5.5 uIU/ml
hGH	0.05	NA	NA	NA	NA	NA	NA	0.82	0–4.7 ng/ml
IGF-1	210.8	272.3	112.6	NA	NA	NA	NA	152.6	49–642 ng/ml
LH/FSH	3.1/6.3	5.5/3.5	NA	NA	NA	NA	0.1>/1.8	1.2/1.5	LH: 0–10.6 uIU/ml FSH: 0.1–9 uIU/ml
ACTH	9.9	NA	NA	NA	NA	NA	88.3	34.8	0–60 pg/ml
Estradiol	39	2.95	NA	NA	NA	0.11	NA	<0.01	Estradiol: 10–441 pg/ml
Testosterone**									Testosterone: 2.79–8.76 ng/ml

* Reference cDNA sequence: NM_001104631.

as on the family members of the Korean patients (both parents and a brother of patient 1; mother and a sister of patient 2; and both parents of patient 8). After identifying the causative gene, exomes of 3 unrelated Japanese patients were also analyzed.

2.2.1. Exome sequencing

2.2.1.1. Library construction. Each sample that was sequenced was prepared according to Illumina protocols. Briefly, 1 μg of genomic DNA was fragmented by nebulization, the fragmented DNA was repaired, an 'A' was ligated to the 3′ end of fragments, Illumina adapters were then ligated to the fragments, and the samples were size selected, aiming for products of 350–400 base pairs. The size-selected products were amplified using PCR, and each final product was validated using Agilent Bioanalyzer. Before first hybridization, multiple libraries with distinct indices were combined into a single pool and then enrichment. The pooled DNA libraries were mixed with the "capture" probes against the targeted regions and incubated for the recommended hybridization time, which ensured that the targeted regions bound completely to the capture probes. Streptavidin beads were used to capture the probes bound to the targeted regions and the beads were washed thrice to remove non-specifically bound DNA. The enriched library was then eluted from the beads and prepared for a second hybridization. The DNA library obtained from the first elution was mixed with the capture probes against the target regions, and the second hybridization ensured that the targeted regions were enriched further. Streptavidin beads were used again to capture the probes containing the targeted regions and the beads were washed thrice to eliminate non-specifically bound DNA. The library thus enriched was eluted from the beads and prepared for sequencing. PCR was used to amplify the enriched DNA library for sequencing. PCR was performed using the same PCR primer cocktail used in TruSeq DNA Sample Preparation. Axeq Technologies conducted quality-control analysis on the sample library and quantified the DNA library templates.

2.2.1.2. Clustering and sequencing. Illumina used a unique "bridged" amplification reaction that occurs on the surface of the flow cell. A flow cell containing millions of unique clusters was loaded into HiSeq 2000 for automated cycles of extension and imaging.

2.2.1.3. Extension and imaging. Solexa's Sequencing-by-Synthesis used 4 proprietary nucleotides possessing reversible fluorophore and termination properties. Each sequencing cycle occurred in the presence of all 4 nucleotides, leading to a higher accuracy than with methods where a single nucleotide at a time is present in the reaction mix. This cycle was repeated, one base at a time, generating a series of images, each representing a single base extension at a specific cluster.

2.2.1.4. Sequence analysis. Paired-end sequences produced by HiSeq 2000 were mapped to the human genome, where the reference sequence was the UCSC assembly hg19 (NCBI build 37), without unordered sequences and alternate haplotypes; the mapping program used was BWA (version 0.5.9rc1). Uniquely mapped reads were only included for the latter steps. After generating a consensus sequence by creating a pileup file from the BAM file, a variant-calling process was run using SAM tools (version 0.1.12a), at which stage candidate SNPs and short indels were detected at nucleotide resolution. These variants were then annotated using ANNOVAR (version 2011Jun18) based on functional predictions, including SIFT and PolyPhen, to filter SNPs from the dbSNP for versions of 131 and 132, and to search SNPs from the 1000 Genomes project. Finally, in-house scripts and open programs were used to estimate various numbers obtained from all stages.

For consistency, the PDE4D residue numbering that we adopt here is based on the reference PDE4D4 isoform (GenBank accession No. NP_001098101) because the Leiden Open Variation Database (LOVD) of human Mendelian genetic variation uses human PDE4D4 (NP_001098101) as the reference sequence.

2.2.2. Sanger sequencing

Genomic DNA was extracted from peripheral blood leukocytes using Wizard Genomic DNA Purification kit, following the manufacturer's instructions (Promega). *PDE4D* exons and their flanking introns were amplified using primer sets we designed (available upon request). PCR was performed using a thermal cycler (model 9700, Applied Biosystems) as follows: 32 cycles of denaturation at 94 °C for 30 s, annealing at 60 °C for 30 s, and extension at 72 °C for 30 s. After treating the amplicon (5 μL) with 10 U of shrimp alkaline phosphatase and 2 U of exonuclease I (USB Corporation), direct sequencing was performed using a BigDye Terminator Cycle Sequencing Ready Reaction kit (Applied Biosystems) on an ABI Prism 3130xl genetic analyzer (Applied Biosystems). Novel *PDE4D* variants were confirmed on more than 2000 ethnicity-matched control chromosomes by sequencing. To describe sequence variations, we followed the guidelines of the Human Genome Nomenclature Committee (HGVS); the 'A' of the ATG translation start site was numbered +1 in DNA sequences and the first methionine was numbered +1 in protein sequences.

2.3. Functional studies

The disease-associated mutants are denoted as per PDE4D4 as the LOVD of human Mendelian genetic variation using human PDE4D4 (NP_001098101) as the reference sequence. This particular isoform is not widely expressed and is found predominantly in the brain [47]. We, have thus made and functionally characterized these mutations in the commonly expressed PDE4D5 isoform [47].

To predict the structural change in PDE4D mutations, molecular modeling and docking simulation of wild-type (WT) and mutant PDE4D were conducted, and we tested whether overexpression of recombinant WT or mutant PDE4D5 proteins affects the intracellular cAMP levels in HEK293 cells after treating with the adenylyl cyclase activator, forskolin.

Next, we measured the cAMP-hydrolyzing activity of the PDE4D mutant in Epstein–Barr virus (EBV)-transformed lymphocytes from patient 8 (with *PRKAR1A* p.R368* mutation) and patient 6 (with *PDE4D* p.L230S mutation), and we determined the phosphorylated Cyclic AMP Response Element-Binding Protein (pCREB):CREB ratio in the patient cells by Western blotting. We also measured total PDE and PDE4-specific activity to determine whether *PDE4D* mutations affect cAMP hydrolysis in the EBV-immortalized lymphocytes from the patients and control subjects. We determined the total cAMP-hydrolyzing activity in the presence or absence of the pan-PDE inhibitor IBMX, which inhibits all cAMP-hydrolyzing PDEs except PDE8 [8]. We also conducted these assays in the presence of the PDE4-specific inhibitor rolipram [8–11] to estimate the PDE4 fraction of total PDE activity. Lastly, we measured the expression of PDE4 and its isoforms in the patient cells and control cells.

2.3.1. Molecular modeling and docking simulation of wild-type and mutated PDE4D

We built 3D structural models for the catalytic domain of the PDE4D wild-type (WT) and its 2 mutants (p.Gly673Asp and p.Ile678Thr; based on PDE4D4). In PDB, several X-ray structures of PDE4D are available, and their overall structures are similar to each other and display a conserved shape for the cAMP-binding pocket. For 3D modeling, we employed a recently proposed high-accuracy template-based modeling method [48]. This method based on global optimization was shown to be successful in recent CASP7 and CASP8 protein-structure prediction experiments [49–51]. A total of 9 templates were used as core templates (3G4G, 1ZKN, 1OYN, 1ROR, 3LY2, 3G4I, 2QYK, 3DYN, and 2OUR), and 4 additional templates were used in a combinatorial manner (2H44, 1TBF, 3JWQ, and 3ITU) to consider 16 possible template combinations. The

final 3D model of each target sequence was selected from among 1600 candidate models by assessing their quality and comparing their structure with the X-ray structure of WT PDE4D (3G4I). The final models were all similar to 3G4I, with backbone RMSDs being approximately 0.4 Å (0.4×10^{-10} m). To estimate the binding affinity between the protein 3D models and cAMP, we performed docking simulations by using AutoDock Vina [52], a new and improved version of AutoDock. We performed flexible docking by considering these 14 flexible side-chains around the cAMP-binding pocket of PDE4D4: D503, D620, Q671, N623, G673 (D673 for p.Gly673Asp), I678 (T678 for p.Ile678Thr), Y461, H462, H466, H502, M575, L621, I638, and F642. A total of 30 exhaustive docking simulations were performed for each protein model.

2.3.2. CREB phosphorylation assay

For Western blotting analysis of phosphorylated-CREB levels in cells, EBV-transformed lymphocytes or HEK293 cells were harvested, washed with phosphate buffered saline (PBS), and lysed in RIPA buffer. Proteins were quantified using the BCA assay (Pierce). Equal amounts of whole cell lysates were separated using SDS-polyacrylamide gel electrophoresis (SDS-PAGE) and transferred to nitrocellulose membranes. Western blotting was performed using antibodies against CREB phosphorylated at Ser133 (pCREB) and total CREB (Cell Signaling Technology). Blots were developed using a peroxidase-conjugated secondary antibody and ECL Plus Western Blotting Detection System (Amersham™).

2.3.3. Quantification of cAMP

The cAMP-measuring kit was purchased from R&D Systems (Abingdon); cellular cAMP concentrations were measured using the competitive-binding technique, according to the manufacturer's instructions.

2.4. Generation of PDE4D knockout rats

The PDE4D knockout (KO) rats were generated and provided by Transposagen Biopharmaceuticals (Lexington, KY). $Pde4d^{Tn(sb\text{-}T2/Bart3)2.285Mcwi}$ on an F344 background was produced by a single-gene trap method based on the Sleeping Beauty transposable element [53]. After confirming trap-vector insertion in the 1st intron of *PDE4D*, rats homozygous for the PDE4D-targeted KO mutation were mated and pups were used for further analyses.

3. Results

3.1. Patient profiles and mutations

Seven patients diagnosed as acrodysostosis without hormone resistance were included in the study. The clinical and molecular characteristics of the patients are summarized in Table 1, and detailed mutation profiles and radiographs of patients are presented in Fig. 1A–J. The disease-associated mutants are denoted as per PDE4D4 as the LOVD of human Mendelian genetic variation uses human PDE4D4 (NP_001098101) as the reference sequence [47].

3.2. Three dimensional structure analysis of PDE4D mutants

Analyzing the 3D structure of the PDE4D mutants predicted changes in the binding efficacy of cAMP to the catalytic pocket in PDE4D mutants, indicating diminished enzymatic activity in the mutants (Table 2 and Fig. 2).

Cartoon figures of protein backbone structures (WT, p.Gly673Asp, and p.Ile678Thr; based on PDE4D4) with bound cAMP are shown in superposition in Fig. 2. The 3D models show few structural differences between WT and the 2 mutants in their backbones and side-chains, except for the mutated residues. The 2 mutated residues (p.Gly673Asp and p.Ile678Thr), which are positioned at the right-hand side of the cAMP-binding pocket, are represented by purple stick figures in Fig. 2B. Table 2 shows the average lowest binding affinity in a docking simulation between PDE4D and its substrate, cAMP. We observed that the WT protein was slightly more stable with cAMP, by approximately 0.17 kcal/mol, than the 2 mutants. This is because the WT and mutants have the same conserved binding residues (D503, D620, and Q671) around the cAMP-binding site, according to the Uniprot annotation; consequently, the binding conformations that correspond to the lowest binding energy are nearly identical, with only small variations in side-chain conformation around cAMP (Fig. 2B). The lowest binding energy and the number of successful bindings of each protein model are shown in Table 2. A successful binding corresponds to the formation of appropriate hydrogen bonds between cAMP and the binding residues of each protein (Fig. 2B). The standard deviation was calculated from 30 independent docking simulations. For WT PDE4D, all 30 simulations resulted in the same successful docking conformation that is shown in Fig. 2B. By contrast, the lowest energy binding conformations of the 2 mutants were found only 4 and 9 times out of 30 simulations (Fig. 2B), implying that the mutated residues entropically deter the binding of cAMP to the catalytic pocket and possibly affect enzymatic activity. The multiple sequence alignment used for 3D modeling showed that G673 is conserved and I678 is either conserved or substituted by a similar hydrophobic residue such as Val.

The Gly673Asp mutation results in the small neutral Gly residue in the WT protein being exchanged for a bulky negatively charged Asp residue. This Asp residue in the mutant could potentially interact with the –OH of cAMP and either block or inhibit cAMP entry into the binding pocket, thereby preventing efficient catalysis.

The Ile678Thr mutation exchanges a hydrophobic Ile residue for a hydrophilic Thr residue. Hydrophobic residues generally shield hydrogen bonds that form between the ligand and the protein in the catalytic pocket by providing a protective hydrophobic cap. Therefore, ablation of this hydrophobicity by the replacement with hydrophilic Thr likely interferes with critical internal hydrogen bonds between the protein and cAMP, and could therefore attenuate effective catalysis.

3.3. Functional studies on PDE4D mutants

PDE4D encodes a series of isoforms generated through the use of alternative promoters and alternative mRNA splicing. These isoforms are characterized by unique N-terminal regions that are invariably employed to target them to specific signaling complexes in cells, thereby conferring the unique functionality of the PDE4D isoforms [7,19]. The reference PDE4D isoform, PDE4D4 isoform is not widely expressed and is found predominantly in the brain [47]. We, have thus made and functionally characterized these mutations in the commonly expressed PDE4D5 isoform [47].

We assessed the functional activity of the Gsα-cAMP-PKA signal transduction pathway in the cells by measuring cAMP hydrolysis and the phosphorylation status of CREB, which is a pivotal target for PKA action. PDE4D5 is a common PDE4D long isoform responsible for desensitizing cAMP signals that arise from Gs-coupled cell-surface receptors [54]. We analyzed whether overexpressing recombinant WT or mutant PDE4D5 proteins affects intracellular cAMP levels in HEK293 cells treated with forskolin, which activates adenylyl cyclase. Whereas overexpressing WT PDE4D5 markedly lowered forskolin-stimulated cAMP levels, overexpressing Q228P-, G673D-, and I678T-PDE4D5 mutants at similar expression levels did not (Fig. 3A).

Next, we measured the cAMP-hydrolyzing activity of PDE4D mutants in EBV-transformed lymphocytes from patient 8 (with *PRKAR1A* p.R368X mutation) and patient 6 (with *PDE4D* p.L230S mutation). The cAMP level in the cells from patient 6 was significantly lower at 30 min after treatment with forskolin when compared to the cells from the control subject ($P = 0.02$, Fig. 3B).

Western blotting demonstrated that the pCREB to CREB ratio was significantly decreased in the cells from both patients 6 and 8 when

compared with the cells from the control subject (Fig. 3C and D): the basal level of pCREB in EBV-transformed cells from both patients was lower than in the control cells (Fig. 3C), and, after a 30-min treatment with forskolin, lower levels of pCREB were detected in the cells from the patients than in control (Fig. 3D). All cells had similar total CREB levels (Fig. 3B and D).

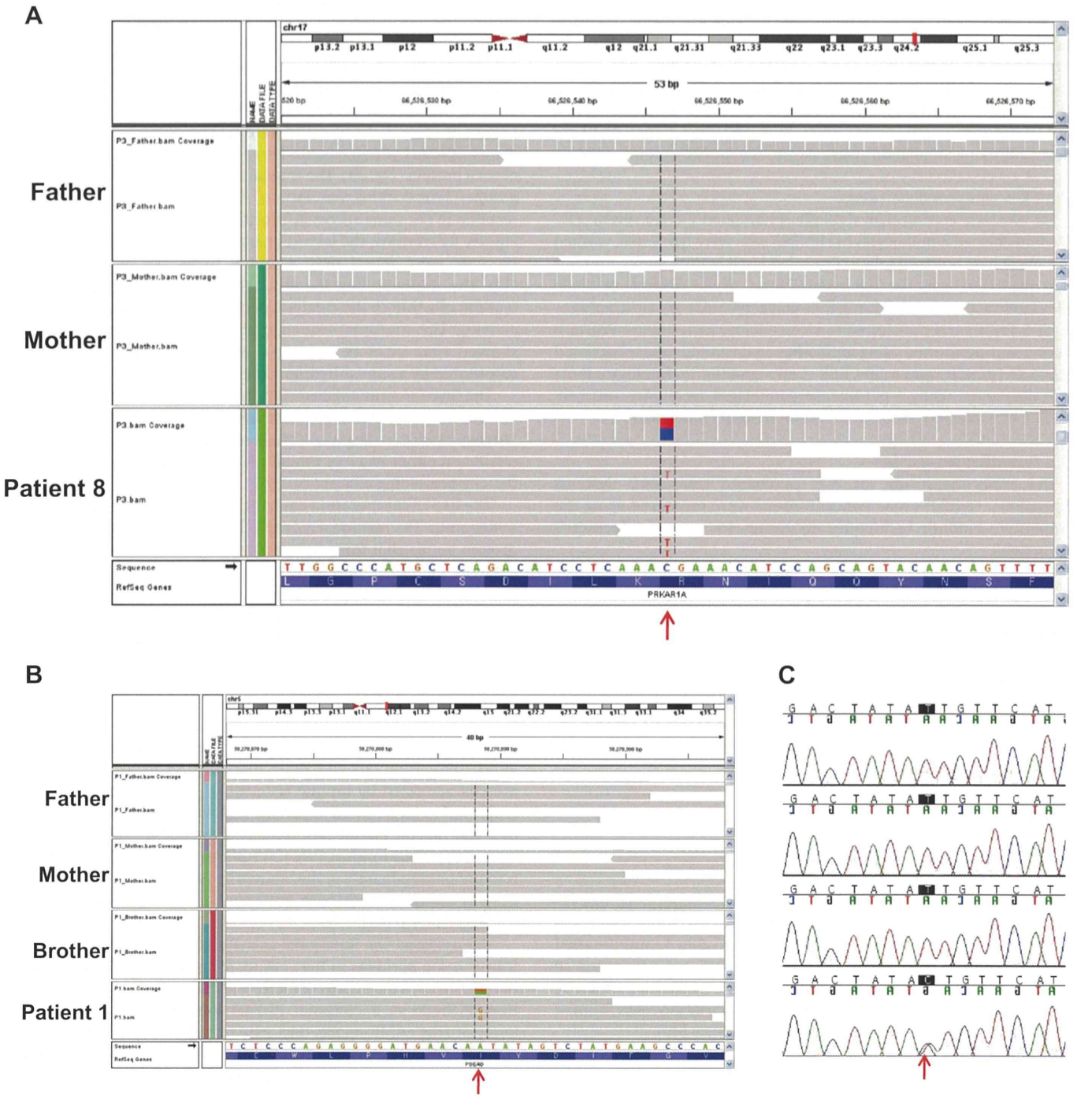

Fig. 1. Identification and confirmation of *PRKAR1A* and *PDE4D* mutations. A; The IGV browser view of the *PRKAR1A* gene region from the exome sequencing data shows that patient 8 (bottom panel) has the c.1101C > T (p.Arg368X) mutation in the *PRKAR1A* gene (arrow), but the father (top panel) and mother (middle panel) have the WT sequence. B; The IGV browser view of the *PDE4D* gene region from the exome sequencing data shows that patient 1 (bottom panel) has the c.2033 T > C (p.Ile678Thr) mutation in the *PDE4D* gene (arrow), but the father (top panel), mother (upper middle panel), and brother (lower middle panel) have the WT sequence. C; Sanger sequencing confirmed that patient 1 has a heterozygous mutation (c.2033 T > C; p.Ile678Thr) in the *PDE4D* gene (arrow), whereas the other family members have WT sequences. D; The IGV browser view of the *PED4D* gene region from the exome sequencing data shows that patient 2 (bottom panel) has the c.2018G > A (p.Gly673Asp) mutation in the *PDE4D* gene (arrow), but the mother (top panel) and sister (middle panel) have the WT sequence. E; Sanger sequencing confirmed that patient 2 has a heterozygous mutation (c.2018G > A; p.Gly673Asp) in the *PDE4D* gene (arrow), whereas the other family members have WT sequences. F; A comparison of the protein sequences of human, chimpanzee, orangutan, dog, mouse, and zebra fish orthologs of PDE4D shows that p.Gly673 and p.Ile678 are highly conserved residues. G; The IGV browser view of the *PED4D* gene region from the exome sequencing data shows that patient 4 (upper panel) and patient 5 (lower panel) have the c.683A > C (p.Gln228Pro) mutation in the *PDE4D* gene (arrow). H; Sanger sequencing confirmed that patients 4 and 5 have a heterozygous mutation (c.683A > C; p.Gln228Pro) in the PDE4D gene (arrow). I; Schematic diagram and Sanger sequencing of 3 mutations detected in the *PDE4D* genes in patients 6, 7, and 3. Mutations are indicated on a PDE4D protein structure with conserved domains. P: phosphorylation sites. UCR: upstream conserved region. J; X-ray views of hands and feet of patients 1, 2, and 8 revealing typical characteristics of acrodysostosis: shortening of the metacarpals, metatarsals, phalanges, and cone-shaped epiphyses. Patients 1 and 2 showed more severe bony abnormalities than patient 8.